



Contents lists available at [ScienceDirect](https://www.sciencedirect.com)

Spectrochimica Acta Part A: Molecular and Biomolecular Spectroscopy

journal homepage: www.elsevier.com/locate/saa



Short Communication

Red/NIR neutral BODIPY-based fluorescent probes for lighting up mitochondria

Jian Yang^{a,1}, Ran Zhang^{b,1}, Yue Zhao^a, Jiangwei Tian^{b,*}, Shifa Wang^a, Claude P. Gros^{c,*}, Haijun Xu^{a,*}

^aJiangsu Co-Innovation Center of Efficient Processing and Utilization of Forest Resources, Jiangsu Provincial Key Lab for the Chemistry and Utilization of Agro-forest Biomass, College of Chemical Engineering, Nanjing Forestry University, Nanjing 210037, China

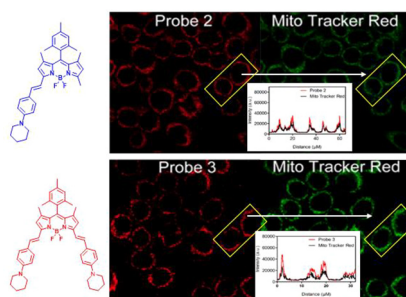
^bState Key Laboratory of Natural Medicines, Jiangsu Key Laboratory of TCM Evaluation and Translational Research, School of Traditional Chinese Pharmacy, China Pharmaceutical University, Nanjing 211198, China

^cICMUB (UMR CNRS 6302), Université Bourgogne Franche-Comté, 21000 Dijon, France

HIGHLIGHTS

- Two probes based on BODIPY scaffolds were prepared by one step reaction.
- Photophysical characterizations and applications in biological imaging were performed.
- The two probes show excellent mitochondrial targeting ability.

GRAPHICAL ABSTRACT



ARTICLE INFO

Article history:

Received 5 September 2020

Received in revised form 29 October 2020

Accepted 5 November 2020

Available online xxxx

Keywords:

BODIPY

Mitochondria

Fluorescent probes

Imaging

ABSTRACT

Two mitochondrial-targeted fluorescent probes, **2** and **3**, based on a BODIPY scaffold and one or two piperidinyl groups were easily synthesized by Knoevenagel condensation. The biological imaging applications of the two probes **2** and **3** in live HepG2 cells reveal that these two probes display excellent mitochondrial imaging ability. Thus, these probes appear as promising tools for visualization of mitochondrial within live cells.

© 2020 Elsevier B.V. All rights reserved.

1. Introduction

Mitochondria are double-membrane enveloped organelles that exist in almost all types of eukaryotic cells [1]. Mitochondria not only provide energy to cells by generating Adenosine TriPhosphate (ATP) but they are also responsible for producing cellular Reactive

Oxygen Species (ROS), initiating cellular apoptosis, regulating cell proliferation and cell cycle [2–4]. Cell damage can induce changes in the sizes and the structures of mitochondria [5,6]. Furthermore, mitochondria play crucial roles in regulating cell metabolism, calcium concentration, apoptosis and human cancers, and any damage or disorder in mitochondria can result in serious human diseases such as cancer, neurodegeneration, cardiovascular dysfunction or Alzheimer Diseases (AD) [3,7–9]. Nowadays, considerable efforts have been dedicated to the study of abnormal functions of mitochondria in biomedical research [10,11]. However, large number of cellular activities, mitochondrial functions

* Corresponding authors.

E-mail addresses: jwtian@cpu.edu.cn (J. Tian), Claude.Gros@u-bourgogne.fr (C.P. Gros), xuhaijun@njfu.edu.cn (H. Xu).

¹ These authors contributed equally to this work.

<https://doi.org/10.1016/j.saa.2020.119199>

1386-1425/© 2020 Elsevier B.V. All rights reserved.

and related mechanisms are still unclear [3,12]. Thus, the development of an effective approach that can accurately monitor the change of the mitochondrial morphologies is of great significance to better understand physiological and pathological functions on mitochondrion in subcellular levels, both *in vitro* and *in vivo*. Fluorescence imaging has emerged as one of the highly useful and powerful methods to monitor and visualize bioprocesses in real time due to its high sensitivity, excellent selectivity, non-invasion, as well as real-time and high spatial resolution imaging in living cells or organisms. The visualization of mitochondrial morphology by live-cell imaging techniques have therefore attracted broad interests because of providing useful information for biochemical cellular processes and diagnosis of various diseases' conditions under the cellular level [5,12–14]. Therefore, various types of mitochondria-selective fluorescent probes have been developed and used successfully to observe the morphology of mitochondria *via* cell imaging techniques [15–17]. However, some mitochondrial fluorescent probes suffer from undergoing difficult post-modification of the molecular scaffold [18–20]. Furthermore, cationic probes are chemically unstable and may also induce cytotoxicity by *e.g.* imposing mitochondrial membrane depolarization, which further limits their applications in living cell studies [3,21]. Consequently, it is highly necessary and of high interest to design neutral or noncationic mitochondria targeted fluorescent probes with high affinity and selectivity.

Recently, BODIPY derivatives have been regarded as one of the most popular family of fluorescent dyes in the field of bioimaging owing to their main advantages such as good photophysical properties, excellent chemical stability and good biocompatibility [5,22–25]. Neutral BODIPY derivatives have proved to be good substitutes of cationic probes to target mitochondria [5,10,26–31]. However, to the best of our knowledge, there are only a few reports on the use of neutral BODIPY derivatives as fluorescent probes to target mitochondria [3,21]. Considering all these facts, we intended to develop neutral, easy-to-synthesize and cost-effective fluorescent probes for tracking mitochondria *via* live cell imaging techniques. In the current study, we wish to report two neutral mitochondria-targeted fluorescent probes, namely green-BODIPY **2** and blue-BODIPY **3** (Scheme 1), by combining one or two piperidinyl units to a BODIPY fluorophore *via* C = C double bonds. This way, the piperidinyl groups are used to guide the BODIPY dye into mitochondria, while maintaining BODIPY its attractive fluorescent properties. In contrast to many other staining probes that require extensive and/or complicated routes for their synthesis, compounds **2** and **3** were readily prepared in a moderate yield but *via* a simple two-steps sequence. The added piperidinyl group is used as a recognition moiety. The synthetic route to access BODIPY dyes **2** and **3** is shown in Scheme 1 and follow our previous report [32]. The chemical structures of compounds **2** and **3** were fully characterized by ¹H NMR, ¹³C NMR, ¹⁹F NMR, MALDI-TOF MS and elemental analysis (Fig. S2–S9, online). Interestingly, the two probes display characteristics of mitochondria staining probes.

2. Materials and methods

2.1. Materials

All chemicals and solvents were of analytical reagent grade and used directly as received unless otherwise noted. Solvents for reactions were purified and dried according to standard procedures, and then distilled before use. Dichloromethane (99.8%) was purchased from Sinopharm Chemical Reagent Co. and fresh distilled before use for electrochemistry. All reagents for synthesis were commercially available and used directly without further purification. All mixtures of solvents are given in *v/v ratio*.

2.2. Cell culture and imaging

HepG2 cells were cultured in Dulbecco's modified Eagle medium (DMEM) supplemented with 10% fetal bovine serum (FBS), penicillin (80 U mL⁻¹), and streptomycin (80 μg mL⁻¹) at 37 °C in a cell incubator containing 5% CO₂ and 95% air. For cell imaging, HepG2 cells (4 × 10⁴/well) were seeded into 35-mm confocal dishes to grow for 24 h. Cells were imaged with a confocal laser scanning microscope (CLSM, LSM800, Zeiss, Germany) with a 63 × oil objective lens.

2.3. Cytotoxicity assay

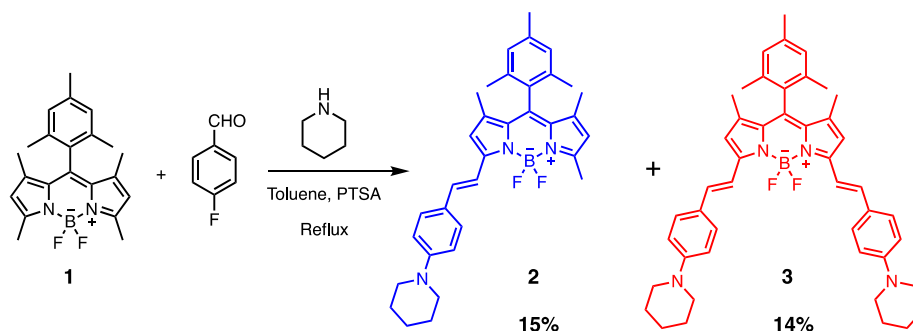
To investigate the cytotoxicity of probes **2** and **3**, standard methyl thiazolyl tetrazolium (MTT) assay was used to determine their biocompatibility. In brief, HepG2 cells (4 × 10³/well) with good condition were seeded into a 96-well plate in 200 μL DMEM *per well* and cultured in the incubator at 37 °C overnight. After rinsing with PBS, HepG2 cells were incubated with serial concentrations of probe **2**, probe **3**, Mito Tracker Green and Mito Tracker Red (200 μL/well) for 24 h, respectively. Then, cells were treated with 200 μL of MTT working solution (0.5 mg/mL) for another 4 h. After discarding the MTT working solution, 150 μL of DMSO was added to each well to dissolve the formazan. Afterwards, the optical density (OD) value was recorded at the wavelength of 570 nm and reference wavelength of 650 nm with a microplate reader after 10 mins of shaking. The cell viability was then determined as follows: Cell viability (%) = (OD₁-OD₂)/(OD₃-OD₂) × 100, where OD₁ represented OD value of treatment group, OD₂ represented OD value of blank group, and OD₃ was OD value of control group.

2.4. Cellular uptake assay

The cellular uptake assay was carried out using CLSM imaging. HepG2 cells (4 × 10⁴/well) were seeded into 35-mm confocal dishes to grow fully in incomplete high sugar medium for 24 h in an incubator. Media was removed and HepG2 cells were washed with phosphate buffered saline (PBS). A 10 μM for probe **2** or 20 μM for probe **3** in serum-free medium was added, and cells were then incubated for different time (0.25 h, 0.5 h, 1 h, 2 h, 4 h). Meanwhile, the cells were stained with Hoechst 33,342 (25 μg/mL) for 0.5 h, then cells were rinsed with PBS three times to perform cell imaging using a CLSM. The signal of Hoechst 33,342 was excited at 405 nm with a helium–neon laser and collected at 420–480 nm. Probes **2** and **3** were excited at 639 nm with an argon ion laser and collected at 650–720 nm. All images were treated and analyzed by a ZEN 2012 imaging software.

2.5. Colocalization experiments

A 10 μM solution of probe **2** in serum-free medium was added into the confocal dish to incubate for 2 h in the humidified incubator. Commercial fluorescent dyes were used to analysis localization of the probe. Hoechst 33,342 was used to stain cell nucleus, Lyso Tracker Green was used to stain lysosome, ER Tracker Green was used to stain endoplasmic reticulum and Mito Tracker Green was taken to track mitochondria. Hoechst 33,342 (25 μg/mL), Lyso Tracker Green (4 μM), ER Tracker Green (4 μM) or Mito Tracker Green (5 μM) were added to incubate for 0.5 h, respectively, then cells were washed with PBS three times before cell imaging was carried out. Afterwards, cells were visualized using a CLSM with fixed parameters, such as the laser intensity, objective lens, exposure time and so on. The signal of Hoechst 33,342 was excited at 405 nm and received at 420–480 nm. Lyso Tracker Green, ER Tracker Green and Mito Tracker Green were both excited at



Scheme 1. Synthesis of BODIPY dyes **2** and **3**.

488 nm and collected at 495–540 nm. Probes **2** was excited at 639 nm and received at 650–720 nm. The colocalization experiments of probe **3** was consistent with that of probe **2** mentioned above, except that the concentration of probe **3** was 20 μM .

3. Results and discussion

3.1. Cytotoxicity assay

In order to investigate the biocompatibility of probes **2** and **3**, the classical MTT method was utilized to measure their half-maximal inhibitory concentrations (IC_{50}). Considering the absorption of probe **2** at 570 nm, we removed the background absorbance. Moreover, we have chosen two usual mitochondrial markers to carry out MTT tests and compared their IC_{50} with probes **2** and **3**. The results showed that when incubated with

probe **2** (100 μM) and probe **3** (80 μM) for 24 h, the cell viability of HepG2 cells remained almost 75% and 80% (Fig. S1a-b), indicating the good biocompatibility of probes **2** and **3**. Moreover, IC_{50} of Mito Tracker Red and Mito Tracker Green were 5.05 μM and 3.36 μM , respectively (Fig. S1c-d).

3.2. Cell uptake of probe **2** and **3**

To track the cell uptake and further explore the optimal incubation time of probes **2** and **3**, HepG2 cells were stained with probes **2** and **3** at different times (0, 0.25, 0.5, 1, 2, 4 h) and imaged by confocal fluorescence imaging. As shown in Fig. 1 for probe **2** and Fig. 2 for probe **3**, with the incubating time increasing from 0 to 4 h, the fluorescence intensity increased gradually for the first two hours, then remained at a high level and tended to be intense and stable for another two hours.

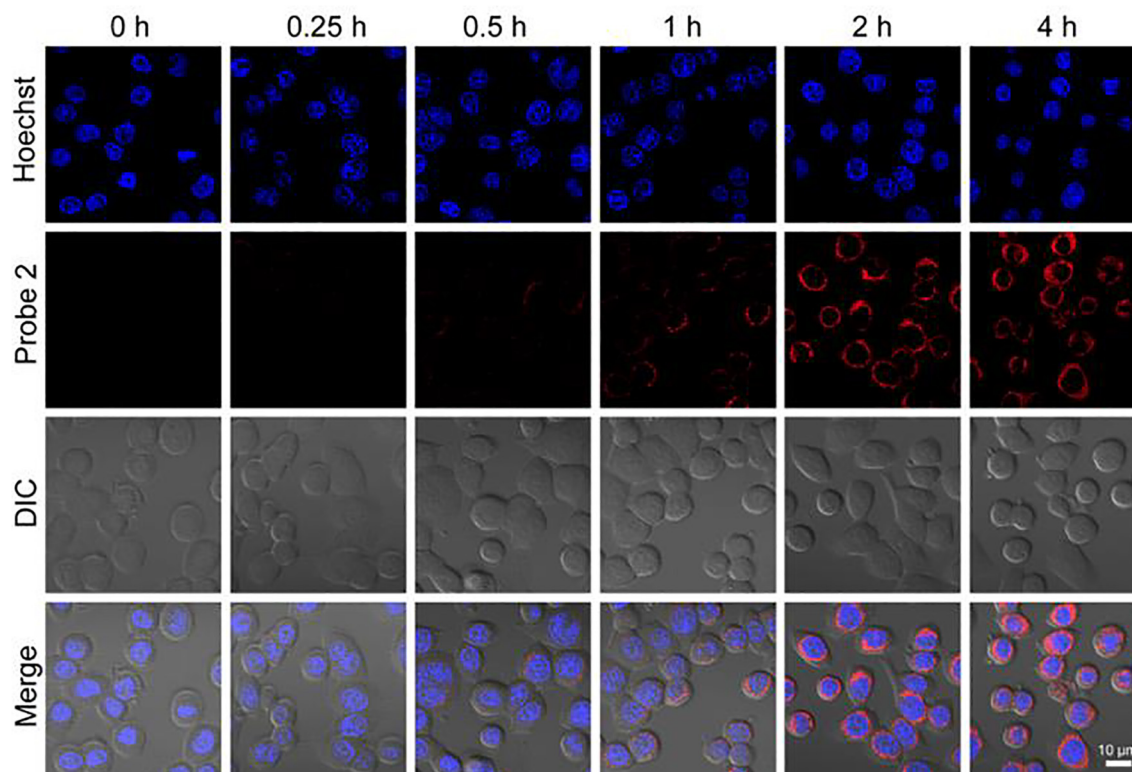


Fig. 1. Confocal fluorescence imaging of HepG2 cells stained with probe **2** (10 μM , excited at 639 nm and collected at 650–720 nm) and Hoechst 33,342 dye (25 $\mu\text{g}/\text{mL}$, excited at 405 nm and collected at 420–480 nm) at different incubating times at 37 $^{\circ}\text{C}$. Scale bars: 10 μm .

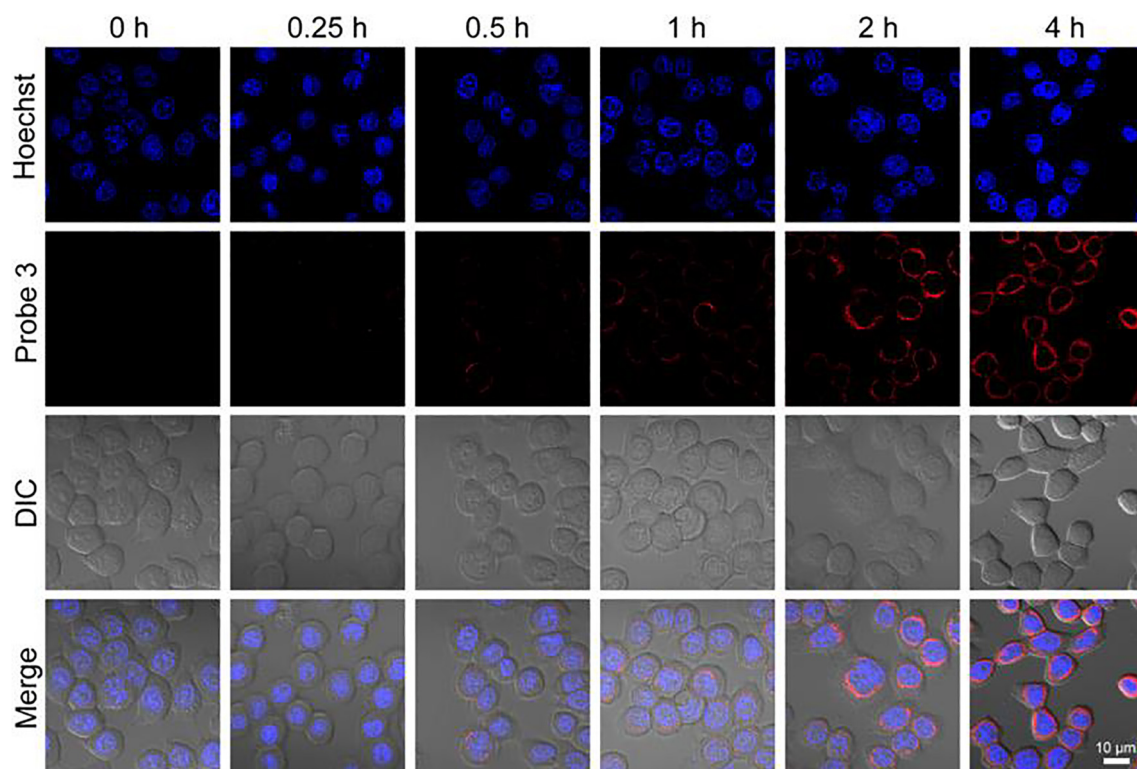


Fig. 2. Confocal fluorescence imaging of HepG2 cells stained with probe **3** (20 μM , excited at 639 nm and collected at 650–720 nm) and Hoechst 33,342 (25 $\mu\text{g}/\text{mL}$, excited at 405 nm and collected at 420–480 nm) at different incubating times at 37 $^{\circ}\text{C}$. Scale bars: 10 μm .

3.3. Colocalization analysis of living cells

In order to further confirm the targeting properties of probes **2** and **3**, colocalization experiments were carried out in living cells with CLSM. After incubating HepG2 cells with probe **2**, Hoechst 33342, Lyso Tracker Green, ER Tracker Green or Mito Tracker Green, the fluorescence image of probe **2** could be fully displayed in cancer cells with probe **2** incubation for 2 h. As can be seen from the overlap diagram of probe **2** with nucleus, lysosome, endoplasmic reticulum and mitochondria, probe **2** had a good overlap with mitochondria (Pearson's correlation coefficient: 0.91), but no overlap with nucleus, lysosome and endoplasmic reticulum (Fig. 3a). In addition, mitochondrial targeting specificity of probe **2** was further verified by linear Regions Of Interest (ROI) analysis. The ROI of probe **2** and Mito Tracker Green showed a consistent trend in fluorescence intensity. In contrast, a poor overlay was visualized between the fluorescence of probe **2** and Lyso Tracker Green (Pearson's correlation coefficient: 0.44), probe **2** and ER Tracker Green (Pearson's correlation coefficient: 0.47), indicating that probe **2** could selectively target mitochondria in living HepG2 cells (Fig. 3b–e and Supplementary Videos 1–4 online). More importantly, this probe had NIR characteristics which not only can prominently reduce background fluorescence, but can also deeply penetrate tissues to allow *in vivo* imaging [26].

As for probe **3**, its co-localization experiments were in accordance with probe **2**. In brief, all commercial dyes and incubation time were the same as probe **2** except the concentration of probe **3**. Collected fluorescence images revealed that HepG2 cells were marked with probe **3** successfully, suggesting that probe **3** had also great cell membrane permeability as probe **2**. Furthermore, in order to investigate the subcellular localization of probe **3**, the overlay figures of probe **3** with Hoechst 33342, Lyso Tracker Green, ER Tracker Green and Mito Tracker Green respectively showed that

probe **3** only overlapped well with the mitochondrial dye. No colocalization was observed in the nucleus, lysosome, or endoplasmic reticulum (Fig. 4a). To further quantify the colocalization effect of probe **3**, Pearson sample correlation factors were used. The intensity changes of the corresponding plot (mitochondrial and probe **3** costaining) showed a high value of 0.89, whereas the intensity profile between lysosome dye and probe **3** (Pearson's correlation coefficient: 0.34), probe **3** and ER Tracker Green (Pearson's correlation coefficient: 0.42) tended to be out of sync (Fig. 4b–e and Supplementary Videos 5–8 online). The above results might be due to the weak polarity of mitochondria, which led to the accumulation of probes **2** and **3** in mitochondria rather than lysosomes or endoplasmic reticuli that are more polar. Moreover, all these phenomena confirmed that probes **2** and **3** were both accumulated in mitochondria, making them suitable as indicators of mitochondria since they displayed higher quantum yields. The photostability of compound **2** and **3** in DCM (Fig. S3 and Fig. S4) and in cellular imaging (Fig. S5) was also investigated. The results showed that the probes were photostable during cellular imaging. Therefore, they may further have wide applications in biological sensing, imaging, and photodynamic therapy [33].

4. Conclusion

In summary, the targeting property of probes **2** and **3** was performed by confocal fluorescence imaging in HepG2 cells. Collected fluorescence images showed that the fluorescence intensity of probes **2** and **3** increased gradually and then tend to be stable with the incubation time developing, suggesting that probes **2** and **3** were entirely internalized into cells and accumulated in subcellular compartments. Confocal fluorescence microscopy revealed that probes **2** and **3** both selectively accumulated in mitochondria in living HepG2 cells. No colocalization was observed in the nucleus

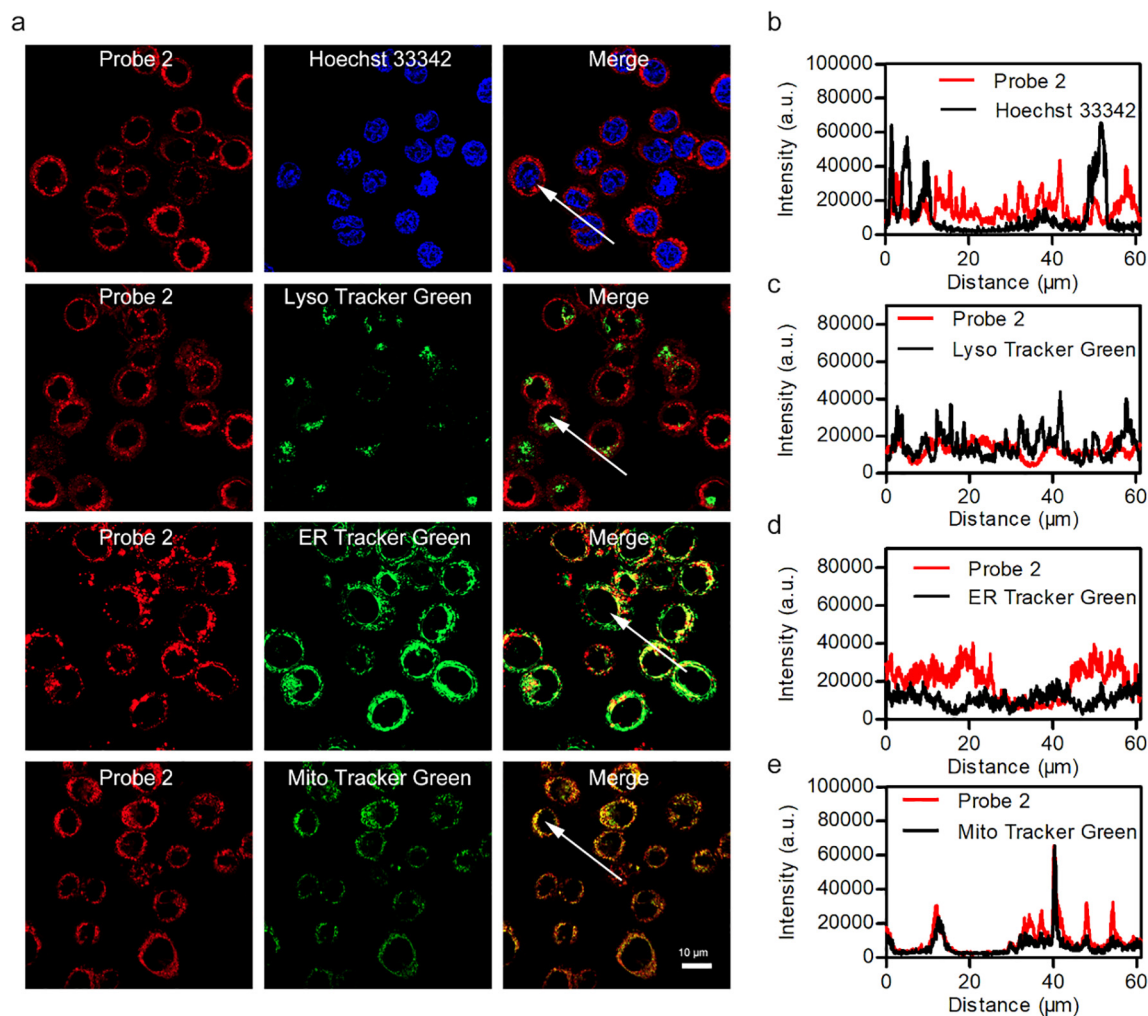


Fig. 3. Targeting property of probe 2. (a) Confocal fluorescence images of HepG2 cells incubated with probe 2 (10 μM , excited at 639 nm and collected at 650–720 nm) for 2 h at 37 $^{\circ}\text{C}$ following staining with Hoechst 33,342 (25 $\mu\text{g}/\text{mL}$, excited at 405 nm and collected at 420–480 nm), Lyso Tracker Green (4 μM , excited at 488 nm and collected at 495–540 nm), ER Tracker Green (4 μM , excited at 488 nm and collected at 495–540 nm) or Mito Tracker Green (5 μM , excited at 488 nm and collected at 495–540 nm) for 0.5 h. Intensity profile of ROI across HepG2 cells of overlap diagrams of nucleus (b), lysosome (c), endoplasmic reticulum (d) and mitochondria (e) with probe 2 respectively. Scale bars: 10 μm .

or lysosome. The two probes displayed excellent mitochondrial targeting ability, which could be further used to visualize mitochondrial fluctuations in live cells. Finally, although the mechanism of targeted mitochondria still needs to be further studied, this study also may provide new strategies for the future design and fabrication of highly efficient mitochondria-targeted fluorescent probes.

Author Statements

Jian Yang and Yue Zhao have contributed to the synthesis and spectroscopic analysis. Ran Zhang and Dr. Jiangwei Tian have contributed for cell imaging investigation and writing of the original draft. Dr. Shifa Wang contributed for the data curation. Prof. Dr. Claude P. Gros and Prof. Dr. Hai-Jun Xu contributed for the supervision, writing of the original draft, and writing-review & editing. The manuscript was well discussed by all of these authors.

Declaration of Competing Interest

The authors declare no conflict of interests.

Acknowledgments

Financially supported by Natural Science Foundation of Jiangsu Province, P. R. China (No. BK20151513, BK20180026), National Natural Science Foundation of China (No.21775166, 21301092), and Postgraduate Research & Practice Innovation Program of Jiangsu Province (KYCX20_0865). JY is thankful to the French Ministry of Research for a PhD grant. This work was supported by the CNRS (UMR UB-CNRS 6302) and the “Université Bourgogne Franche-Comté”.

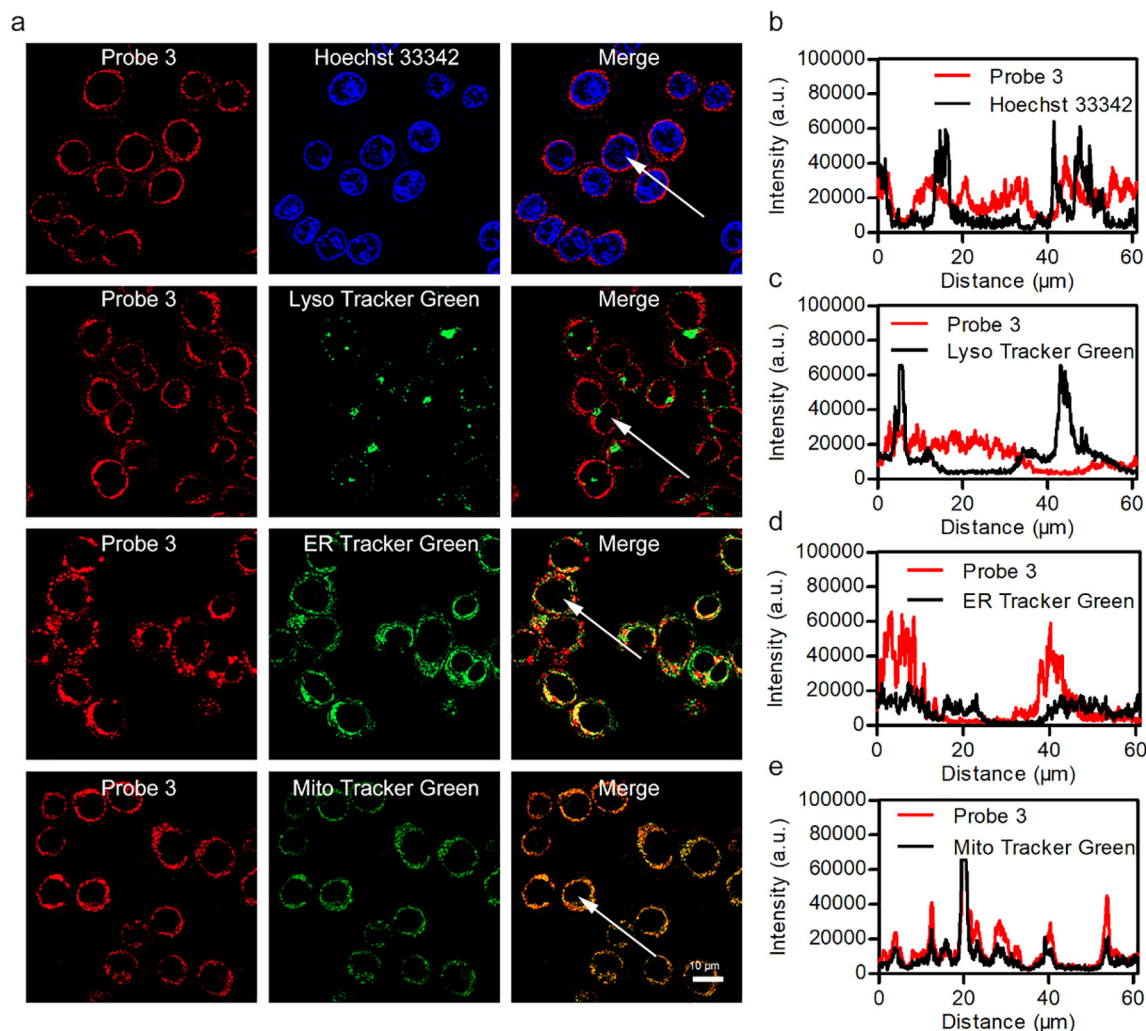


Fig. 4. Targeting property of probe **3**. (a) Confocal fluorescence images of HepG2 cells incubated with probe **3** (20 μM , excited at 639 nm and collected at 650–720 nm) for 2 h at 37 $^{\circ}\text{C}$ following staining with Hoechst 33,342 (25 $\mu\text{g}/\text{mL}$, excited at 405 nm and collected at 420–480 nm), Lyso Tracker Green (4 μM , excited at 488 nm and collected at 495–540 nm), ER Tracker Green (4 μM , excited at 488 nm and collected at 495–540 nm) or Mito Tracker Green (5 μM , excited at 488 nm and collected at 495–540 nm) for 0.5 h. Intensity profile of ROI across HepG2 cells of overlap diagrams of nucleus (b), lysosome (c), endoplasmic reticulum (d) and mitochondria (e) with probe **3** respectively. Scale bars: 10 μm .

Appendix A. Supplementary material

Supplementary data to this article can be found online at <https://doi.org/10.1016/j.saa.2020.119199>.

References

- [1] J. Sun, M. Tian, W. Lin, A two-photon excited red-emissive probe for imaging mitochondria with high fidelity and its application in monitoring mitochondrial depolarization via FRET, *Analyst* 144 (2019) 2387–2392.
- [2] J.R. Friedman, J. Nunnari, Mitochondrial form and function, *Nature* 505 (2014) 335–343.
- [3] P.E. Kesavan, V. Pandey, M.K. Raza, S. Mori, I. Gupta, Water soluble thioglycosylated BODIPYs for mitochondria targeted cytotoxicity, *Bioorg. Chem.* 91 (2019) 103139.
- [4] D.C. Wallace, A mitochondrial paradigm of metabolic and degenerative diseases, aging, and cancer: a dawn for evolutionary medicine, *Annu. Rev. Genet.* 39 (2005) 359–407.
- [5] T. Gao, H. He, R. Huang, M. Zheng, F.-F. Wang, Y.-J. Hu, F.-L. Jiang, Y. Liu, BODIPY-based fluorescent probes for mitochondria-targeted cell imaging with superior brightness, low cytotoxicity and high photostability, *Dyes Pigm.* 141 (2017) 530–535.
- [6] D. Lee, M.-K. Jung, J. Yin, G. Kim, C.-G. Pack, J. Yoon, An aniline bearing hemicyanine derivative serves as a mitochondria selective probe, *Dyes Pigm.* 136 (2017) 467–472.
- [7] T. Bek, Mitochondrial dysfunction and diabetic retinopathy, *Mitochondrion* 36 (2017) 4–6.
- [8] Y. Lei, L. Liu, X. Tang, D. Yang, X. Yang, F. He, Sanguinarine and chelerythrine: two natural products for mitochondria-imaging with aggregation-induced emission enhancement and pH-sensitive characteristics, *RSC Adv.* 8 (2018) 3919–3927.
- [9] S. Vyas, E. Zaganjor, M.C. Haigis, Mitochondria and cancer, *Cell* 166 (2016) 555–566.
- [10] B. Sui, S. Tang, A.W. Woodward, B. Kim, K.D. Belfield, A BODIPY-based water-soluble fluorescent probe for mitochondria targeting, *Eur. J. Org. Chem.* 2016 (2016) 2851–2857.
- [11] J. Zielonka, J. Joseph, A. Sikora, M. Hardy, O. Ouari, J. Vasquez-Vivar, G. Cheng, M. Lopez, B. Kalyanaraman, Mitochondria-targeted triphenylphosphonium-based compounds: syntheses, mechanisms of action, and therapeutic and diagnostic applications, *Chem. Rev.* 117 (2017) 10043–10120.
- [12] P.E. Porporato, N. Filigheddu, J.M.B. Pedro, G. Kroemer, L. Galluzzi, Mitochondrial metabolism and cancer, *Cell Res.* 28 (2018) 265–280.
- [13] G. Masanta, C.S. Lim, H.J. Kim, J.H. Han, H.M. Kim, B.R. Cho, A mitochondrial-targeted two-photon probe for zinc ion, *J. Am. Chem. Soc.* 133 (2011) 5698–5700.
- [14] A.C. Shaikh, M.E. Varma, R.D. Mule, S. Banerjee, P.P. Kulkarni, N.T. Patil, Ionic pyridinium-oxazole dyads: design, synthesis, and application in mitochondrial imaging, *J. Org. Chem.* 84 (2019) 1766–1777.
- [15] R. Mayank, A. Rani, N. Singh, N. Garg, N. Kaur, Singh, Mitochondria- and nucleolus-targeted copper(I) complexes with pyrazole-linked triphenylphosphine moieties for live cell imaging, *Analyst* 145 (2019) 83–90.
- [16] T. Zhang, C. Yin, Y. Zhang, J. Chao, G. Wen, F. Huo, Mitochondria-targeted reversible ratiometric fluorescent probe for monitoring SO_2/HCHO in living cells, *Spectrochim. Acta A Mol. Biomol. Spectrosc.* 234 (2020) 118253.
- [17] Y. Shen, L. Dai, Y. Zhang, H. Li, Y. Chen, C. Zhang, A novel pyridinium-based fluorescent probe for ratiometric detection of peroxynitrite in mitochondria, *Spectrochim. Acta A Mol. Biomol. Spectrosc.* 228 (2020) 117762.

- [18] L. Hu, B. Fang, L. Hu, Y. Shen, S. Hussain, J. Liu, T. Liu, S. Wang, Q. Zhang, Y. Tian, X. Tian, A small molecule emitting in the near infrared region with pH sensitivity for visualization mitochondria under super-resolution microscopy, *Talanta* 199 (2019) 140–146.
- [19] D. Su, C.L. Teoh, N. Gao, Q.H. Xu, Y.T. Chang, A simple BODIPY-based viscosity probe for imaging of cellular viscosity in live cells, *Sensors (Basel)* 16 (2016).
- [20] H. Wang, B. Fang, L. Xiao, D. Li, L. Zhou, L. Kong, Y. Yu, X. Li, Y. Wu, Z. Hu, A water-soluble “turn-on” fluorescent probe for specifically imaging mitochondria viscosity in living cells, *Spectrochim. Acta A Mol. Biomol. Spectrosc.* 203 (2018) 127–131.
- [21] T. Gayathri, S. Karnewar, S. Kotamraju, S.P. Singh, High affinity neutral BODIPY fluorophores for mitochondrial tracking, *ACS Med. Chem. Lett.* 9 (2018) 618–622.
- [22] L. Fu, F.-F. Tian, L. Lai, Y. Liu, P.D. Harvey, F.-L. Jiang, A ratiometric “two-in-one” fluorescent chemodosimeter for fluoride and hydrogen sulfide, *Sens. Actuat., B* 193 (2014) 701–707.
- [23] L. Fu, F.-F. Wang, T. Gao, R. Huang, H. He, F.-L. Jiang, Y. Liu, Highly efficient fluorescent BODIPY dyes for reaction-based sensing of fluoride ions, *Sens. Actuat., B* 216 (2015) 558–562.
- [24] T. Kowada, H. Maeda, K. Kikuchi, BODIPY-based probes for the fluorescence imaging of biomolecules in living cells, *Chem. Soc. Rev.* 44 (2015) 4953–4972.
- [25] J. Yang, Y. Fan, F. Cai, X. Xu, B. Fu, S. Wang, Z. Shen, J. Tian, H. Xu, BODIPY derivatives bearing borneol moieties: Enhancing cell membrane permeability for living cell imaging, *Dyes Pigm.* 164 (2019) 105–111.
- [26] N. Jiang, J. Fan, T. Liu, J. Cao, B. Qiao, J. Wang, P. Gao, X. Peng, A near-infrared dye based on BODIPY for tracking morphology changes in mitochondria, *Chem. Commun.* 49 (2013) 10620–10622.
- [27] X. Kong, F. Su, L. Zhang, J. Yaron, F. Lee, Z. Shi, Y. Tian, D.R. Meldrum, A highly selective mitochondria-targeting fluorescent $K^{(+)}$ sensor, *Angew. Chem. Int. Ed. Engl.* 54 (2015) 12053–12057.
- [28] L.L. Li, K. Li, M.Y. Li, L. Shi, Y.H. Liu, H. Zhang, S.L. Pan, N. Wang, Q. Zhou, X.Q. Yu, BODIPY-based two-photon fluorescent probe for real-time monitoring of lysosomal viscosity with fluorescence lifetime imaging microscopy, *Anal. Chem.* 90 (2018) 5873–5878.
- [29] S. Nigam, B.P. Burke, L.H. Davies, J. Domarkas, J.F. Wallis, P.G. Waddell, J.S. Waby, D.M. Benoit, A.M. Seymour, C. Cawthorne, L.J. Higham, S.J. Archibald, Structurally optimised BODIPY derivatives for imaging of mitochondrial dysfunction in cancer and heart cells, *Chem. Commun.* 52 (2016) 7114–7117.
- [30] T. Xiong, M. Li, X. Zhao, Y. Zou, J. Du, J. Fan, X. Peng, Functional two-photon cationic targeted photosensitizers for deep-seated tumor imaging and therapy, *Sens. Actuat., B* 304 (2020).
- [31] H. Zhu, J. Fan, J. Du, X. Peng, Fluorescent probes for sensing and imaging within specific cellular organelles, *Acc. Chem. Res.* 49 (2016) 2115–2126.
- [32] R. Sharma, D. Volyniuk, C. Popli, O. Bezikonny, J.V. Grazulevicius, R. Misra, Strategy toward tuning emission of star-shaped tetraphenylethene-substituted truxenes for sky-blue and greenish-white organic light-emitting diodes, *J. Phys. Chem. C* 122 (2018) 15614–15624.
- [33] L. Yuan, W. Lin, K. Zheng, L. He, W. Huang, Far-red to near infrared analyte-responsive fluorescent probes based on organic fluorophore platforms for fluorescence imaging, *Chem. Soc. Rev.* 42 (2013) 622–661.